BioMACROMOLECULES

Article

pubs.acs.org/Biomac

Fabrication of Endothelial Cell-Laden Carrageenan Microfibers for Microvascularized Bone Tissue Engineering Applications

Silvia M. Mihaila,[†,‡] Elena G. Popa,[†,‡] Rui L. Reis,[†,‡] Alexandra P. Marques,[†,‡] and Manuela E. Gomes*[,†,‡]

[†]3B's Research Group − Biomaterials, Biodegradables and Biomimetics, University of Minho, Headquarters of the European Institute of Excellence on Tissue Engineering and Regenerative Medicine, AvePark, 4806-909 Taipas, Guimarães, Portugal

[‡]ICVS/3B's − PT Government Associate Laboratory, 4710-243 Braga, Guimarães, Portugal

Supporting Information

ABSTRACT: Recent achievements in the area of tissue engineering (TE) have enabled the development of three-dimensional (3D) cell-laden hydrogels as in vitro platforms that closely mimic the 3D scenario found in native tissues. These platforms are extensively used to evaluate cellular behavior, cell−cell interactions, and tissue-like formation in highly defined settings. In this study, we propose a scalable and flexible 3D system based on microsized hydrogel fibers that might be used as building blocks for the establishment of 3D hydrogel constructs for vascularized bone TE applications. For this purpose, chitosan (CHT) coated κ-carrageenan (κ-CA) microfibers were developed using a two-step procedure involving ionotropic gelation (for the fiber formation) of κ-CA and its polyelectrolyte complexation with CHT (for the enhancement of fiber stability). The performance of the obtained fibers was assessed regarding their swelling and stability profiles, as well as their ability to carry and, subsequently, promote the outward release of microvascular-like endothelial cells (ECs), without compromising their viability and phenotype. Finally, the possibility of assembling and integrating these cell-laden fibers within a 3D hydrogel matrix containing osteoblast-like cells was evaluated. Overall, the obtained results demonstrate the suitability of the microsized κ-CA fibers to carry and deliver phenotypically apt microvascular-like ECs. Furthermore, it is shown that it is possible to assemble these cell-laden microsized fibers into 3D heterotypic hydrogels constructs. This in vitro 3D platform provides a versatile approach to investigate the interactions between multiple cell types in controlled settings, which may open up novel 3D in vitro culture techniques to better mimic the complexity of tissues.

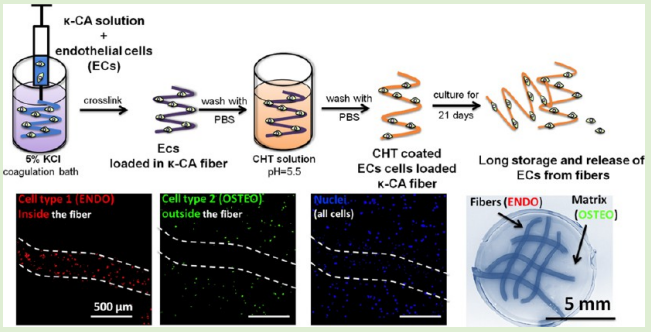

1. INTRODUCTION

In the past decade, tissue engineering (TE) has emerged as a multidisciplinary field at the interface of medicine, biology, and engineering, aiming at fabricating tissue-like biological constructs.[1] However, the lack of a vasculature that can sustain the nutrients and oxygen demands within the tissue-engineered construct is a major limiting factor in creating thick artificial tissues.[2] Thus, developing vessel-like networks based on endothelial cells (ECs), as integrated templates within TE constructs,[3] would be essential for creating real-size replicas of tissues or organs.[4,5]

Hydrogels have been proven to provide ideal mimics of cellular matrices, as their hydrated state resembles that of native extracellular matrix (ECM),[6] and their high permeability to oxygen, nutrients, and metabolites diffusion[7] enables cell encapsulation. Additionally, natural-origin hydrogels showed high potential in the TE field, due to their chemistry and properties similar to ECM.[8] Several processing methodologies such as prototyping/printing,[9] microfluidics,[10] and photolitography[11] have been used to develop vessel-like architectures based on ECs-loaded hydrogels that exhibit microsized features (~50 μm[11] to 1 mm[9]). However, these methods often require sophisticated equipment and elaborated experimental settings and reagents that frequently raise concerns over their cytotoxicity.[12,13]

Wet spinning of hydrogels is a very simple and straightforward method, requiring minimal laboratorial utensils and short processing time. The wet spinning of hydrogel fibers involves the extrusion of a polymer solution through a needle into a coagulation bath that triggers the cross-linking of the polymer into a fiber-like shape. This methodology has been successfully used to develop hydrogel fibers based on several natural-origin polymers, such as alginate,[14] collagen,[15] gellan gum,[16] chitosan,[17] or a combination of carrageenan and alginate.[18]

Carrageenans (CAs) stand out, among other natural-origin polymers, as potential candidates for TE applications, due to their mild gelation properties and resemblance to glycosaminoglycans (GAGs), main components of the ECM of biological systems. CAs are highly sulfated linear polysaccharides with alternating repeating 3,6-anhydro-D-galactose and β-D-galactose-

Received: January 9, 2014
Revised: June 18, 2014

   dx.doi.org/10.1021/bm500036a | Biomacromolecules XXXX, XXX, XXX−XXX

4-sulfated units, that provide structural support in several species of marine red algae (class of Rhodophyceae). Due to the half-ester sulfate moieties present on their backbone (their amount determines the type of carrageenan that can be iota, lambda, or kappa), CAs are strong anionic polymers. As a consequence, their gelation occurs by ionic interactions with appropriate counter-ions, such as K^+, Na^+, or Ca^{2+}. Although these hydrophilic polysaccharides have been widely used as emulsifiers, gelling, thickening, or stabilizing agents in the food or pharmaceutical industry,[19] the intrinsic thixotropic behavior of κ-carrageenan (κ-CA), in particular, has justified its exploitation as an injectable matrix for the delivery of living cells[18,20,21] and biomacromolecules.[22,23] However, κ-CA hydrogels exhibit high swelling ratios and mechanical instability in physiological conditions[24] which has motivated the development of several approaches to increase their stability, such as chemical modifications with photo-cross-linkable moieties,[25] blending with other biopolymers,[18,26] addition of nanocomposites to the polymer solution,[23] and formation of interpenetrating networks[27] or polyelectrolyte complexation (PEC) with polycations, such as chitosan (CHT).[28] Numerous studies have reported CHT-based PEC systems with positive outcomes, in terms of stability as well as cellular viability and behavior.[29,30] Electrostatic interactions between κ-CA and CHT have also been used for the development of nanoparticles,[31] beads,[32] and layer-by-layer systems.[33]

The present work reports on the development of κ-CA microfibers coated with CHT using a two-step-procedure, and on their potential as cell carriers and building blocks of 3D constructs for vascularized bone tissue engineering. Therefore, in a first step, κ-CA fibers of various diameters were obtained by wet spinning. In a second step, in order to reinforce the fibers and enhance their stability in physiological relevant microenvironment, κ-CA fibers were coated with CHT, through the electrostatic interaction between the polymers. The obtained fibers were then loaded with microvascular-like ECs obtained from the SSEA-4^+ subpopulation of adipose tissue stromal vascular fraction, as described in a previous study.[34] The phenotype of the ECs was evaluated prior to and after entrapment within the fibers. Ultimately, envisioning a heterotypic 3D bone TE construct with independent and defined microarchitectures, we proposed an innovative 3D buildup of ECs loaded fibers within a hydrogel matrix containing osteoblast-like cells. In summary, this study showed that it is possible to developed cell-laden κ-CA-based hydrogel fibers that exhibit high stability in prolonged culture conditions. Furthermore, these fibers could be stacked in a desired pattern and successfully integrated into a 3D construct.

2. MATERIALS AND METHODS

2.1. Materials. κ-Carrageenan (κ-CA), potassium chloride (KCl), and β-glycerophosphate disodium salt hydrate (βGP) were purchased from Sigma, Germany. Reagent grade medium molecular weight chitosan (CHT) (Sigma, Germany) with a 90% degree of acetylation was used. Prior to use, CHT was purified using a precipitation method.[35] All other reagents were used as received.

2.2. Development of CHT Coated κ-CA Fibers. *2.2.1. Production of κ-CA Fibers through Ionotropic Gelation.* The κ-CA hydrogel fibers were obtained by wet spinning technique, which consisted of the extrusion of the polymer solution through a needle immersed in a coagulation bath, as previously described elsewhere.[18] Briefly, a 1.5% (wt/v) κ-CA solution was prepared by dissolving the polymer in distilled water at 50 °C and under constant stirring until complete dissolution was achieved. Subsequently, the κ-CA solution was loaded into 5 mL syringes and κ-CA fibers with different diameters were obtained by extruding the polymeric solution through needles with different gauges (18G to 27G), directly into a 5% (wt/v) KCl solution prepared in distilled water. The presence of K^+ ions initiated the ionotropic gelation by counterbalancing the negative charges of κ-CA. The fibers were allowed to harden in the coagulation bath for about 10 min, sufficient time for them to retain the shape. Finally, the fibers were washed with phosphate buffered saline (PBS) in order to remove the excess of salt. Fibers obtained with needles of 25G and 27G were selected for all the subsequent assays.

2.2.2. Optimization of the pH of the CHT Working Solution. Chitosan dissolves in acid solutions, which limits its use in the presence of living cells. Previous studies[36] have shown that βGP, a weak base, increases the pH of CHT solutions, without jeopardizing its solubility. Therefore, in order to establish optimal conditions for the incorporation of cells, while enabling PEC, a curve of variation of pH with the addition of βGP to the CHT solution was obtained. For this purpose, a CHT solution was prepared by dissolving CHT in a 1% (v/v) acetic acid solution at a final concentration of 0.5% (wt/v). In order to determine the degree to which the addition of βGP affects the overall charge of CHT solution, zeta potential measurements were performed using a Malvern Zeta Sizer Nano ZS (Malvern Instruments, UK). Each sample was diluted in ultrapure water at a concentration of 0.1% (wt/v) and analyzed at 25 °C for 60 s.

2.2.3. Coating of κ-CA Fibers through Polyelectrolyte Complexation with CHT. The κ-CA fibers, previously obtained by ionotropic gelation, were immersed in the optimized CHT solution (0.5% (wt/v) and pH = 5.5) for 20 min, followed by several washing steps with PBS to remove the excess of CHT. The presence of the CHT coating was evaluated by staining the fibers with Eosin Y (Sigma, Germany). Fibers without coating were used as negative control.

2.3. Physico-Chemical Characterization of the Developed Fibers. *2.3.1. Swelling Kinetics.* The influence of CHT coating on the swelling and stability of the developed κ-CA fibers was determined by evaluating the fibers' water absorption kinetics and diameter variation upon immersion in culture medium for up to 21 days. The culture medium used for this purpose was Dulbecco's Modified Eagle Medium (DMEM, Gibco, USA) supplemented with 10% (v/v) HiFBS (Gibco, USA) and 1% (v/v) antibiotic/antimycotic (penicillin/streptomycin, 100 U/100 μg/mL, Gibco, UK). Envisioning the use of fibers for cell encapsulation/culturing, the experimental parameters were set at physiological temperature (37 °C) and humidified atmosphere with 5% of CO_2. Medium was replenished every 3−4 days. Fibers (n = 3) were retrieved at days 7, 14, and 21, blotted with KimWipe paper to remove the excess of liquid, and weighed (M_W). Sample's final weight (M_{DF}) was determined upon lyophilization. The swelling kinetics was defined as the ratio between the liquid uptake ($M_W - M_{DF}$) and the final dry mass of polymer (M_{DF}), according to eq 1.

$$\text{mass swelling ratio} = (M_w - M_{DF})/M_{DF} \times 100 \quad (1)$$

The final diameter of the hydrogel fibers was also measured applying software-measuring tools (NIH ImageJ software, http://rsbweb.nih.gov/ij/) to at least three micrographs of each sample.

2.3.2. Morphological and Chemical Characterization. Concomitant with the swelling behavior analysis, samples were retrieved for surface morphological evaluation and elemental analysis under a scanning electron microscope (SEM) coupled with energy-dispersive X-ray spectroscopy (EDX/EDS). Briefly, fibers were snap frozen in liquid nitrogen, transferred to microcentrifuge tubes, and freeze−dried overnight. The dried samples were carefully mounted on sample holders using double-sided carbon tape. Before being analyzed by SEM (Nano-SEM FEI Nova 200), the samples were gold sputter coated (Fisons Instruments, sputter coater SC502, UK). Elemental analysis was carried out with an energy dispersive spectrometer (EDAX-Pegasus X4M) on the same samples used for SEM. All observations/image acquisitions and measurements were made at an acceleration voltage of 15 kV.

2.4. Isolation and Endothelial Differentiation of SSEA-4^+hASCs. Human lipoaspirate samples from healthy donors were kindly provided by Hospital de Prelada (Porto, Portugal), under previously established protocols and with the informed consent of the

dx.doi.org/10.1021/bm500036a | Biomacromolecules XXXX, XXX, XXX−XXX

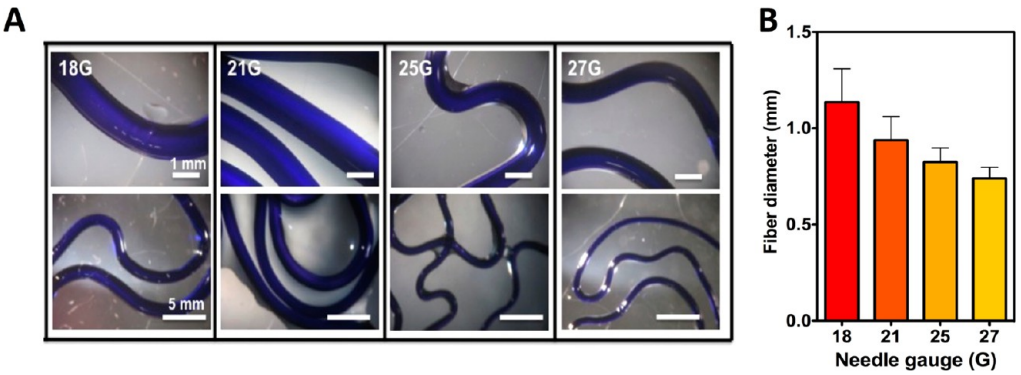

Figure 1. K-CA fibers formed by ionotropic gelation. Needles with different gauges, from 18G to 27G, were used to form the hydrogel fibers. (A) Aspect of fibers using different needle gauges. Staining with methylene blue was performed for contrast purposes. (B) Depending on the needle gauge, fibers diameter spanned from 1.25 mm down to 0.5 mm.

patients. The selection of SSEA-4 positive cells (SSEA-4$^+$hASCs) residing within the stromal vascular fraction of the adipose tissue and differentiation toward the endothelial lineage were performed according to our previously published protocols.[34] Briefly, the SSEA-4$^+$hASCs were selected using immunomagnetic beads (Dynal M-450 Epoxy beads from Dynal Biotech, Carlsbad, CA, USA) coated with SSEA-4 antibody (Abcam, Cambridge, UK). Then, the selected SSEA-4$^+$hASCs cells were differentiated toward endothelial lineage by culturing them for 2 weeks in endothelial cell growth medium, EGM-2 MV (Lonza, Switzerland), containing 5% FBS and supplemental growth factors: hydrocortisone, hFGF-B, ascorbic acid, gentamicin/amphotericin, VEGF, long R3-IGF-1, hEGF, and heparin, at concentrations established by the manufacturer.

2.5. SSEA-4$^+$hASCs-Derived Endothelial Cells Encapsulation within κ-CA Fibers. The κ-CA, CHT, and KCl solutions were sterilized at 120 °C for 30 min. SSEA-4$^+$hASCs-derived ECs at passage 3 were trypsinized and centrifuged, and further suspended in the κ-CA solution at a final cell density of 2×10^6 cells/mL. ECs loaded fibers (with and without CHT coating) were produced as described above. The cell-loaded fibers were then transferred to 24-well plates and maintained in culture in EGM-2 MV for 21 days, at 37 °C in a humidified atmosphere with 5% CO_2. Culture medium was replenished every 3−4 days.

In order to assess the maintenance of the phenotype of the SSEA-4$^+$hASCs derived ECs at 21 days of culture cell-loaded fibers were treated with 0.1% proteinase K (vWR, Portugal) in 1 mM EDTA (Sigma, Germany), 50 mM TrisHCl (Sigma, Germany), and 1 mM iodoacetamide buffer (Sigma, Germany), for 1 h at 37 °C, under constant agitation, to release the cells from the fibers. The cellular pellet recovered after centrifugation (10 min, 400×*g*) was resuspended in EGM-2 MV medium and plated into tissue culture flasks. Cells were cultured until reaching confluence for further analysis, as described below.

2.6. Characterization of the Constructs. *2.6.1. Microscopic Analysis.* Variations in the shape and diameter of the developed cell-loaded fibers (with or without CHT coating), as well as the potential outward migration of the cells to the culture well, were examined using a stereomicroscope (Stemi 1000, Zeiss, Germany) along the time of culture.

2.6.2. Live−Dead Assay. At preselected time culturing points (1, 7, 14, and 21 days), cell-loaded fibers were washed with PBS and incubated with 4 μM calcein-AM (Invitrogen, USA) for 40 min followed by 10 min incubation with 1 μM propidium iodide (PI, Invitrogen, USA). Samples ($n = 3$) were then washed and fixed for 40 min in 10% formalin. After fixation, samples were washed with PBS and cell nuclei were counterstained for 20 min with 4,6-diamidino-2-phenyindole dilactate (DAPI, Sigma, Germany) and then washed three times with PBS. Representative fluorescent micrographs were acquired using the Axioplan Imager Z1 fluorescence microscope (Zeiss, Germany) and the AxioVision 4.8 software (Zeiss, Germany). The quantification of cellular viability was measured by applying software-measuring tools (NIH ImageJ software, http://rsbweb.nih.gov/ij/) to at least three micrographs of each sample.

2.6.3. Flow Cytometry. SSEA-4$^+$hASCs-derived ECs, prior to and after encapsulation, were retrieved from cell culture flasks using TrypLE Express (Invitrogen, USA). 5×10^5 cells were incubated for 30 min at 4 °C with the following markers: CD45-FITC, CD34-PE, CD73-PE, CD31-APC (all from BD Pharmingen, USA), and CD105-FITC and CD90-APC (eBiosciences, USA) at a concentration of 6 μg/mL, as recommended by the manufacturer. After washing with PBS, the cells were resuspended in acquisition buffer (PBS containing 1% formaldehyde and 0.1% sodium azide) and analyzed with a BD FACS-Calibur flow cytometer (BD Biosciences, USA). A minimum of 2×10^5 events was acquired and gated in a forward versus side-scatter dot plot with a linear scale. Results were displayed in histogram plots created using CellQuest software (BD Biosciences, USA). The number of positive events for each cell-specific marker was expressed as a percentage of the total cell number.

2.6.4. Matrigel Assay. SSEA-4$^+$hASCs-derived ECs, at passage 2, were trypsinized and plated at a density of 3×10^4 cells/well in 48-well plates coated with 64 μL of Matrigel (BD Biosciences, USA). Cells were incubated for 4 h at 37 °C. One hour prior fixation, 4 μM calcein-AM (Invitrogen, USA) was added to the wells. Upon fixation, cell nuclei were counterstained with DAPI for 10 min, and then washed three times with PBS. Three representative images were acquired under a fluorescence microscope.

2.7. Assembling the κ-CA Fibers into 3D Hydrogel Discs. Cell-laden fibers containing SSEA-4$^+$hASCs-derived ECs labeled with a GFP tag were transferred to a Petri dish and allowed to settle randomly. A freshly prepared κ-CA solution containing osteogenic differentiated SSEA-4$^+$hASCs (obtained according to a method described elsewhere[34]) and labeled with a rhodamine tag was poured onto the fibers until full coverage. The cross-linking of the κ-CA solution was achieved with a 5% (wt/v) KCl solution. Immediately after cross-linking, the hydrogel disc containing the fibers was fixed with 10% formalin for 40 min. After fixation, the cell nuclei were stained with DAPI for 20 min and observed under a confocal laser scanning microscope (CLSM, Olympus, Fluoview 1000). *YZ* and *XY* projections were performed in order to evaluate the cellular distribution throughout the 3D structures.

2.8. Statistical Analysis. For the swelling ratio and fiber diameter data, statistical analysis was performed using GraphPad Prism 5.00 software (San Diego, USA). Statistical differences ($p < 0.05$) were determined using one-way ANOVA, followed by a Tukey post test.

3. RESULTS AND DISCUSSION

3.1. Different Diameter κ-CA Fibers Formation through Ionotropic Gelation. Cell encapsulation techniques using hydrogels enable the formation of 3D cell-culture models that can potentially replicate tissue organization, which cannot be achieved in conventional 2D cultures.[37] Since the architecture and chemical composition of hydrogels can be easily engineered,

dx.doi.org/10.1021/bm500036a | *Biomacromolecules* XXXX, XXX, XXX−XXX

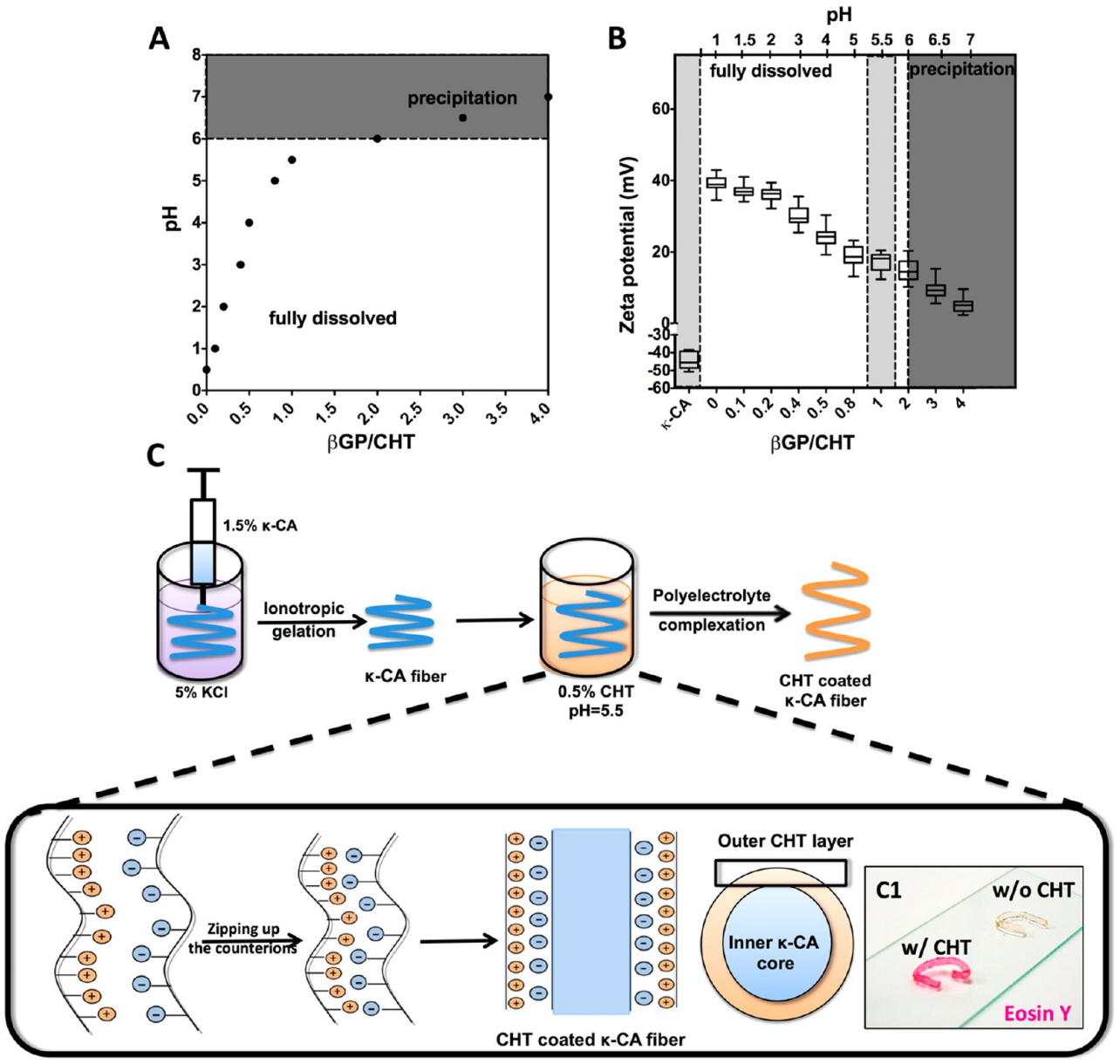

Figure 2. Production of CHT coated κ-CA hydrogel fibers. (A) Variation of the pH relative to the β-glycerophosphate (βGP)/chitosan (CHT) ratio. With the addition of βGP, the CHT solutions reach physiologically relevant conditions (pH 5.5−6). Above this point the precipitation of CHT occurs (dark gray area). (B) With the addition of βGP, the zeta potential of CHT solution is dramatically affected. The zeta potential of κ-CA solutions, measured at pH = 5.5, was used as reference (approximately −40 mV). Values reported correspond to $n = 10$. (C) Schematics of the production of CHT coated κ-CA hydrogel fibers. The process involves the formation of fibers by ionotropic gelation in a KCl coagulation bath, followed by their immersion in an optimized CHT solution. (C1) The presence of the CHT coating was confirmed by staining the fibers with Eosin Y which specifically binds to CHT.

they can be used as tools and platforms to design capture/release of cells in/from 3D tissue-engineered constructs.[38]

Thus, we aimed to develop hydrogel microfibers by making use of a simple and straightforward procedure that enables cell encapsulation in a controlled distribution pattern, without jeopardizing their phenotype and functionality. Among the natural origin polymers, such as alginate,[14,13] collagen,[15] gellan gum,[16,39] or hyaluronic acid[40] that have been used to obtain fibers through wet spinning technique, κ-CA stands out due to its GAG-like features, reversible temperature and ionic gelation properties and intrinsic sheer thinning behavior, particularly thixotropic. This means that upon applied stress the organization of κ-CA chains is disrupted, but it will reset once the deformation is removed.[25] This property renders the use of κ-CA hydrogels as injectable matrixes, as they can be easily extruded through narrow needles without affecting the structure or the entrapped biomacromolecules or cells.[41,42] Taken together, the gelation properties of κ-CA enable the formation of gels in different shapes, including fibers, highlighting therefore the versatility of κ-CA processability.[8]

In the present study, the possibility of producing κ-CA fibers with different diameters was first investigated. To obtain the fiber shape, κ-CA was extruded directly into the coagulation bath, where the cross-linking of the polymer solution occurred. Variation of the diameter depended on the needle gauge used to extrude the κ-CA solution into the coagulation bath (Figure 1A).

dx.doi.org/10.1021/bm500036a | Biomacromolecules XXXX, XXX, XXX−XXX

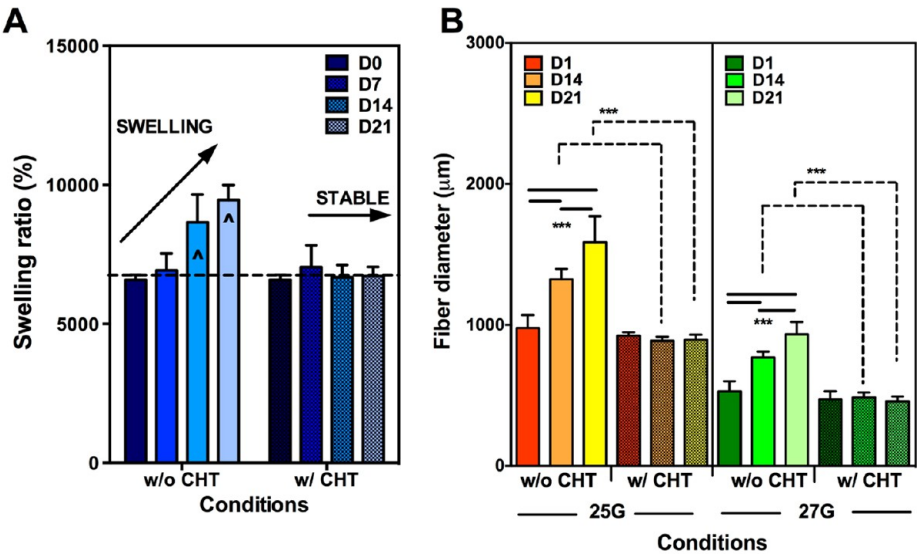

Figure 3. Swelling behavior of κ-CA fibers, without (w/o) and with (w/) CHT coating, in culture medium (DMEM). (A) Swelling ratio increases over time for the fibers without CHT coating. On the other side, the CHT coating stabilizes the hydrogel fibers, hampering their swelling. Values correspond to average ($n = 3$) ± standard deviation. "^" corresponds to a statistical difference ($p < 0.05$) when compared to day 0 and day 7 values of the κ-CA fibers without coating. (B) The diameter of the developed fibers is a direct consequence of the swelling behavior. Thus, the uncoated κ-CA fibers show a significant increase in the fiber diameter along time (***$p < 0.001$), while the diameter of coated fibers remains constant.

Using needle gauges ranging from 18 to 27G, it was possible to obtain fibers with different diameters, directly proportional with the internal diameter of the needles (838−210 μm). The fibers produced within these settings had a diameter ranging from 500 to 1250 μm (Figure 1B), making them appealing for further applications.[13,14,43] These trends were in agreement with previous reports for hydrogel fibers obtained via wet spinning[18] or other techniques.[14]

Taking into consideration that a microsized architecture enables nutrients and oxygen diffusion, crucial for the cellular performance, we decided to further explore the potential κ-CA fibers with the smallest diameters, obtained by the extrusion of κ-CA solutions through the 25G and 27G needles.

3.2. κ-CA Fibers Can Be Coated with CHT through Polyelectrolyte Complexation. Although encouraging results have shown the potential of using κ-CA in TE applications, the ionically cross-linked κ-CA hydrogels exhibit high swelling ratios. It is possible that the culture medium destabilizes the physically cross-linked network, as a result of the uncontrollable and permanent exchange of K^+ ions with other positive ions present in the physiological environment.[24] This allows the inner network to continuously expand, and consequently become loose and mechanically weak.[25,44] If one envisions the prolonged culture periods or the maintenance of initial microfeatures of the hydrogels, such as shape, size, and stability, the reinforcement of the structure is an impetus.

Several methodologies have been employed,[18,25,27] including the formation of polyelectrolyte complexes formed by the ionic interaction between oppositely charged polyelectrolytes. We hypothesized that, by coating the κ-CA hydrogels fibers with CHT, we would be able to stabilize the fibers structure. CHT, a β-1,4-linked D-glucosamine and *N*-acetyl-D-glucosamine, is one of the few positively charged natural-origin polysaccharides and, thus, is widely used as a polycation for the formation of polyelectrolyte complexes. Additionally, its appealing properties such as biocompatibility, biodegradability, low toxicity, and relatively low production cost from abundant sources endorse its use for TE strategies.[45]

Since the amino groups of CHT have a pK_a value of 6.5−6.8,[46] their protonation occurs in acidic solutions with a charge density dependent on pH and degree of acetylation. Besides causing CHT to become water-soluble, the protonated groups can readily bind to the negatively charged groups (carboxylic acid, hydroxyl, or sulfate) of other polymers, to form polyelectrolyte complexes. Thus, our hypothesis was that the protonated amino groups of CHT would bind to the available negatively charged sulfate groups of κ-CA and form an acid−base type of polyelectrolyte complex. Therefore, we have deliberately chosen shorter gelation times for the formation of κ-CA fibers (10 min over standard 30 min[18,41]), so that the fiber shape was retained, without neutralizing all sulfate groups.

However, since the growth of cells is usually optimal when the microenvironment is buffered at a pH in the range 7.2−7.4,[47] the low pH values at which CHT dissolves might compromise their viability. Thus, we explored the possibility of increasing the pH of CHT solutions without jeopardizing their solubility, by adding a week base, βGP,[36] to the solutions. We noticed that, by gradually adding βGP to the CHT solutions, the pH slowly increased without evident signs of precipitation (Figure 2A). Nevertheless, upon reaching the pK_a value, precipitation occurred.

One concern associated with the increase of pH was that the amino groups of CHT would be deionized, which would weaken their binding affinity to the oppositely charged κ-CA, jeopardizing the stability of the layer. To determine whether this was the case, we evaluated the electrical charge of the CHT solution upon addition of βGP, and consecutively upon increase of pH, by measuring the zeta potential. As expected, with the increase of the pH, the overall charge of the CHT solution decreased, though still remaining within the positive range (approximately +10 eV) (Figure 2B). These findings indicate that with the pH modification, the protonation of amino groups still occurs, and consequently CHT would continue to act as a polycation, being suitable for PEC with κ-CA. In the perspective of coating cell-loaded κ-CA fibers, pHof 5.5, where no signs of precipitation were observed and the overall charge of CHT was positive, was considered the most suitable condition.

dx.doi.org/10.1021/bm500036a | *Biomacromolecules* XXXX, XXX, XXX−XXX

A

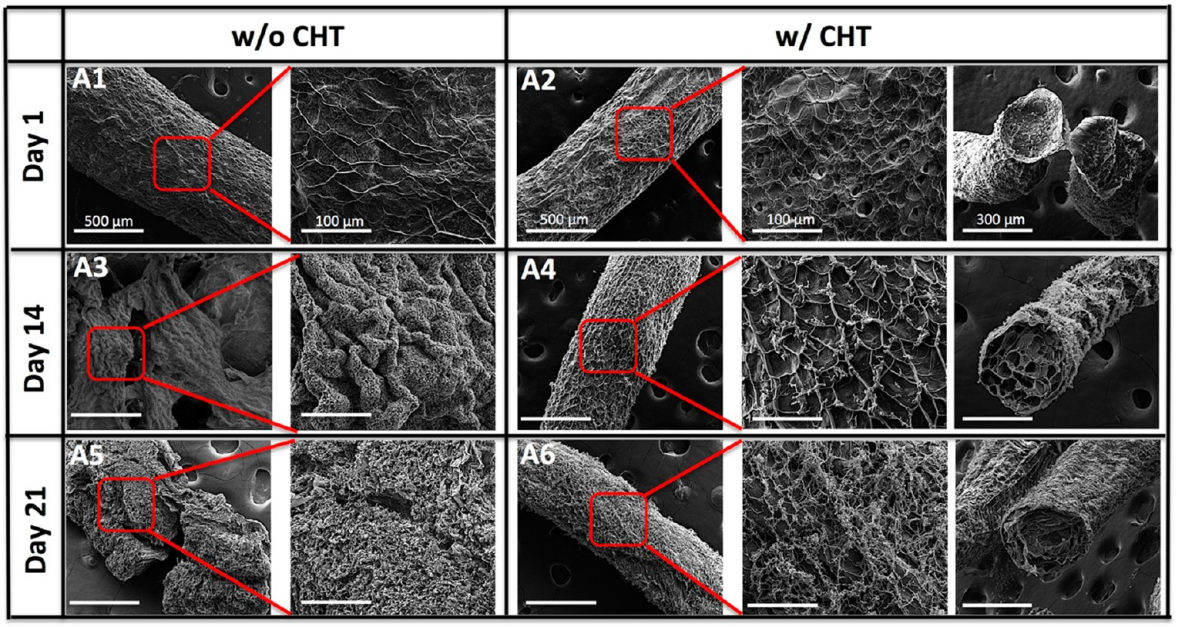

B

Table 1. Elemental composition of κ-CA microfibers with or without CHT coating

Time (days)	EDX/EDS elemental analysis (%wt)						
	Condition	C	O	S	K	Cl	N
1	w/o CHT	26.01	25.82	4.49	9.64	22.32	-
	w/ CHT	35.40	31.67	4.04	1.33	13.19	5.79
14	w/o CHT	31.27	18.8	3.85	7.90	25.15	-
	w/ CHT	41.62	22.38	5.15	1.81	12.04	7.01
21	w/o CHT	41.54	13.5	2.58	1.71	26.67	-
	w/ CHT	24.79	12.88	3.64	1.28	35.25	4.47

Abbreviations: w/o = without; w/ =with.

Figure 4. Physicochemical characterization of the freeze-dried fibers. (A) SEM micrographs depict the alteration of fiber morphology in culture medium (DMEM) over time. The structure of the uncoated fibers is not stable and disintegrates after 21 days (A1-A3-A5), while the CHT coating exhibits a protective role that hinders the disintegration of the fibers and therefore enhances their stability (A2-A4-A6). (B) The presence of CHT was evaluated along time by tracing the amounts of nitrogen (from the $-NH_2$ groups of CHT) present on the surface of the fibers. The element was detected until day 21, suggesting that CHT was still present on the fibers. The defined squares in the SEM micrographs represent the area where the magnification and elemental analysis were performed.

The formation of the polyelectrolyte complexes relies on the interaction between the available negatively charged sulfate groups of κ-CA and the protonated amino groups of CHT (Figure 2C). Thus, the immersion of κ-CA fibers in the optimized CHT solution led to the formation of a localized CHT nanosized layer, which was in agreement with previously published data.[29−33] The presence of the CHT coating was confirmed by the intense pink coloration observed only on the coated fibers after staining with Eosin Y, which specifically stains CHT[48] (Figure 2C−C1 inset). From a practical standpoint, CHT coated fibers, when compared with the uncoated fibers, were easier to separate and handle despite their small diameters.

3.3. CHT Coated κ-CA Fibers Depict Improved Stability.

In the context of TE, it is important to evaluate the behavior of these fibers in conditions similar to the in vivo microenvironment. Swelling properties of hydrogels directly affect the overall features of the polymeric network (shape, size, and mechanical stability). Thus, we aimed to evaluate to which extent the swelling ratio of the developed fibers affects their overall diameter, and whether the presence of CHT provides stability to the fibers. We performed swelling studies by maintaining the coated and uncoated fibers in culture medium, which consists of a collection of ions and proteins that could destabilize the κ-CA hydrogel network.[41]

Our findings showed that the swelling ratios of ionically cross-linked κ-CA fibers significantly increased with time ($p < 0.001$) (Figure 3A). The destabilization of the ionically cross-linked κ-CA network is likely to occur due to the continuous exchange of K^+ ions entrapped within the network with other ions present in the culture medium. In fact, similar results have been reported for ionically cross-linked alginate[24] and gellan gum,[44] where prolonged immersion in culture medium led to the weakening of the network and, consequently, to its collapse.

dx.doi.org/10.1021/bm500036a | Biomacromolecules XXXX, XXX, XXX−XXX

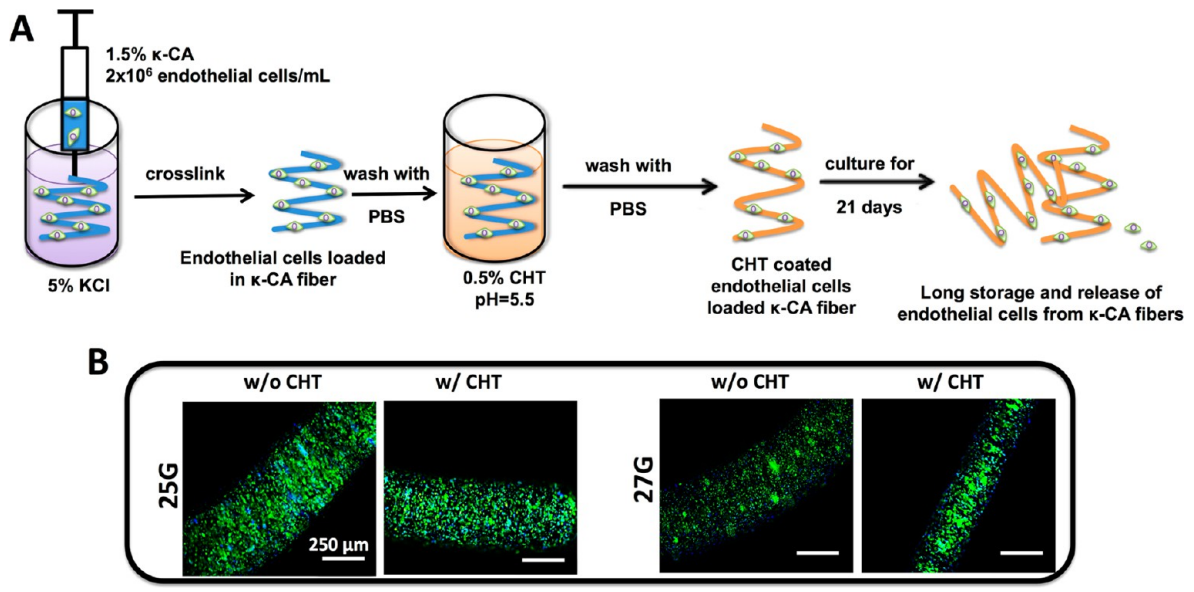

Figure 5. Encapsulation of SSEA-4$^+$hASCs-derived ECs into κ-CA fibers. (A) Schematics of the encapsulation procedure and experimental setup. (B) The assessment of cell viability (live (green)/dead (red)) 24 h after encapsulation shows that the cells were not affected by the processing method, nor by the size and CHT coating of the fibers. Cell nuclei were counterstained with DAPI (blue).

However, CHT coated fibers exhibited a stable swelling ratio over time, significantly inferior to that of the uncoated fibers ($p < 0.001$). This behavior can be due to the strong protective coating layer, preventing the fiber swelling. A similar behavior was described in other studies, concerning the use of CHT in combination with alginate to form a layer of wrapping alginate beads for the controlled release of drugs.[29]

As a consequence, the diameter of CHT coated fibers was maintained constant over time, while the uncoated fibers exhibited an increase in their diameter (Figure 3B). Even more, in terms of manipulation, the uncoated fibers became soft and easy to break, while the coated ones were stable over the long term and easy to handle, without obvious damage to their integrity.

The closer evaluation of the fiber morphology by SEM revealed that the uncoated fibers started to lose their integrity around day 14 (Figure 4A1−3−5), as predicted by the swelling ratio results (Figure 3A). By contrast, the CHT coated fibers exhibited a rougher surface, displaying a mesh-like wrapping around an open-pore κ-CA core. These fibers maintained their shape, size, and integrity until day 21, when small cracks become visible on their surface (Figure 4A2−4−6). The presence of the CHT coating was further demonstrated by tracing the N content on the surface of the CHT-coated κ-CA fibers by EDS/EDX (Figures 4B) over time. Its detection up to 21 days suggested that the CHT-κ-CA electrostatic interactions are strong enough to withstand the presence of other ions and proteins present in the culture medium, leading to a robust and stable structure.

3.4. CHT Coating of the Cell-Loaded κ-CA Fibers Does Not Affect the Endothelial Differentiated SSEA-4$^+$hASCs Phenotype in the Long Term. Recently, several cell types, such as human adipose derived stem cells, human nasal chondrocytes, ATDC5 chondrocytic cell line, and L929 fibroblast cell line, were encapsulated within k-CA hydrogels, processed in different shapes (fibers, beads, discs), with positive results in terms of viability, cellular metabolism, proliferation, and differentiation.[41,49,50] Herein, for the first time, we proposed the encapsulation of microvascular-like ECs within k-CA hydrogel fibers as building blocks of vascularized bone tissue engineered constructs. Pre-vascularization of engineered constructs by using progenitor/endothelial cells has been considered the most promising strategy to address the vascularization of large constructs.[51] However, the use of human cells has been hampered by the limited sources and reduced yields.[52] Our earlier work[34] has shown that the SSEA-4$^+$ subpopulation, selected among the heterogeneous stromal vascular fraction of human adipose tissue, can be differentiated toward both endothelial and osteogenic lineages. Moreover, SSEA-4$^+$hASCs-derived ECs hold features of microvascular ECs that trigger the formation of 3D vascular networks within engineered constructs. Therefore, we have taken advantage of our knowledge to obtain ECs from SSEA-4$^+$ subpopulation (Supporting Information (SI) Figure 1) to develop cell-laden κ-CA-based hydrogel fibers to be used as 3D cellular carriers. SSEA-4$^+$hASCs-derived ECs were encapsulated within the κ-CA and CHT coated κ-CA fibers with 2 different diameters and cultured for a period of 21 days (Figure 5A).

As the encapsulation procedure requires several steps that could lead to reduced cellular performance,[53,54] the direct effect of the experimental conditions over the viability of the encapsulated cells was assessed. Independently of the size and whether fibers were coated or not, the majority of the encapsulated cells were viable (average >65%, SI Figure 2) and homogeneously distributed within the fibers (Figure 5B), suggesting that the production of fibers (ionotropic gelation and PEC) was mild enough.

Additionally, along the culture time and independently of the conditions, viable cells were predominantly observed within the fibers (Figure 6). A slight decrease in cellular viability was noticed, so that by day 21, viable cells comprised 60% of the total cells (SI Figure 2). However, this drop was not as significant as reported in previous studies that associated this outcome with the slow diffusion of nutrients caused by the sample thickness and/or cross-linking mechanism.[25,55,56] It might be due to the fact that fiber-shaped hydrogels were characterized by a larger surface area than disc shaped units, and as a consequence, a faster

dx.doi.org/10.1021/bm500036a | Biomacromolecules XXXX, XXX, XXX−XXX

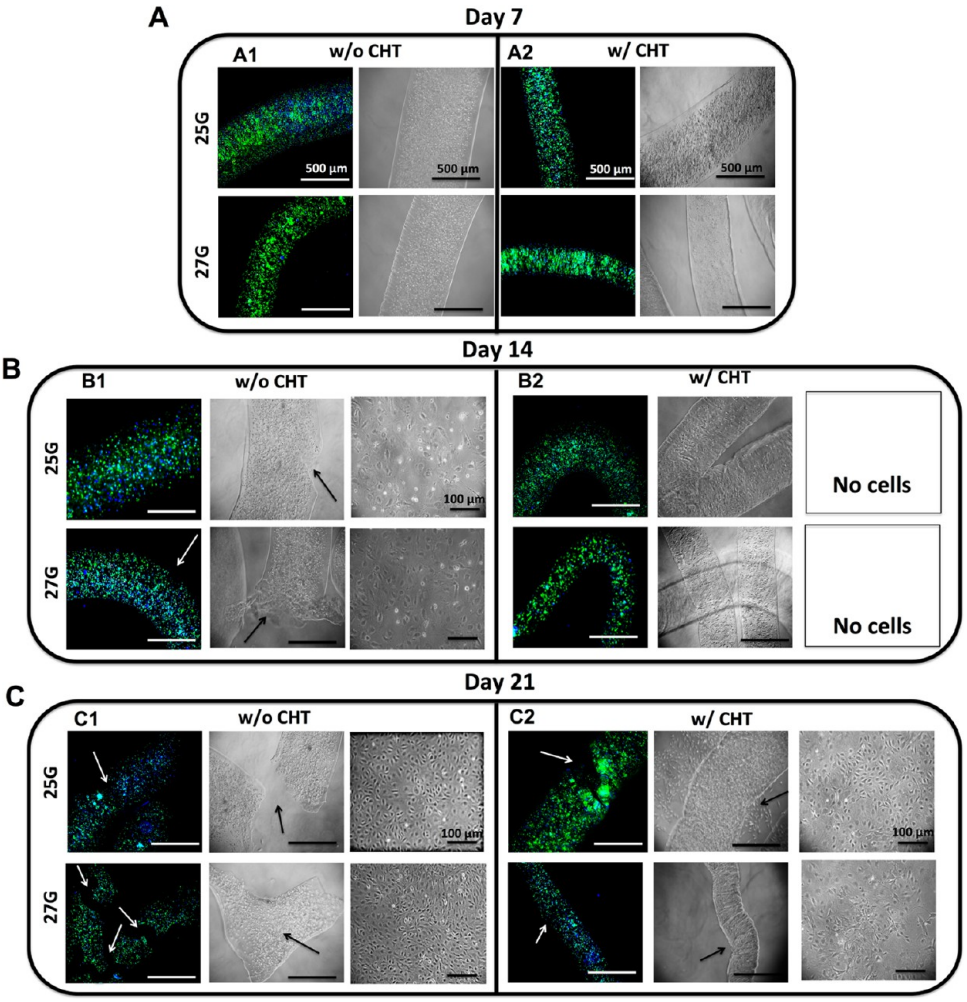

Figure 6. Evaluation of the cell-laden κ-CA hydrogel fibers along 21 days of culture. The viability of encapsulated cells (live/dead/) was maintained during the culture time in all conditions. (A) At day 7, independently of the conditions, fibers were intact, without displaying signs of disintegration. (B1) At day 14, cells escaped the uncoated fibers and small endothelial-like colonies could be observed at the bottom of the well. By day 21 (C1), fibers lose their integrity (arrows), allowing further release of cells into the well plate. Contrarily, the CHT coating (w/CHT) delayed the disintegration of the fibers, hence the release of the cells (B2 and C2). At day 21, the coated fiber diameter did not alter; however, small cracks (arrows) were observed along the fibers allowing the release of the cells. Cell nuclei were counterstained with DAPI (blue).

diffusion of nutrients and oxygen to the core of the sample could occur.[57] It has also been suggested that the ions needed for hydrogel formation may influence the cellular viability; nevertheless, the fibers reported herein are formed via a partial cross-linking process, by shorter exposure times to K^+ treatment than previously reported.[18,58] The additional CHT coating, that was shown to prevent the fibers from swelling, did not affect viability. From the SEM images it was possible to notice that the CHT layer was displayed as a mesh wrapped around the fiber, preventing it from swelling, but enabling diffusion.

The optical analysis of the cell-loaded uncoated fibers showed an increase in their diameter and subsequent disintegration, in agreement with the results obtained with acellular fibers. Concisely, at day 7, uncoated fibers were intact, with a well-delimited smooth surface; however, at day 14, they presented signs of disintegration. This allowed the entrapped cells to "escape" from the fibers and adhere to the well and proliferate (Figure 6A1−C1). In opposition, the CHT coating delayed the disintegration of fibers, as they maintained their initial diameter and their surface did not present disruptions up to day 14 (Figure 6A2−B2). Only at the last time point did small cracks become visible, and consequently, EC colonies were observed on the bottom of the well (Figure 6C2).

Beside potentially affecting cellular viability,[7] cell encapsulation procedures and prolonged culture might also compromise the cell's phenotype or functionality.[20,59] In order to address this question, cells were retrieved from the fibers, after culturing for 21 days, and seeded into tissue culture flasks. Cells were able to adhere and organize into small endothelial-like colonies (Figure 7A) and, more importantly, maintained their ability to form tubular-like structures when seeded on Matrigel (Figure 7B). Moreover, when screened for the initial cell surface marker panel, cells were shown to be $CD105^+/CD73^+/CD31^+/CD34^+/CD45^-/CD90^-$, a signature that matches the one registered prior encapsulation. Taken together, these results show that the encapsulation process, followed by the prolonged culture of cells within fibers and their retrieval, did not affect the phenotype and in vitro functionality of ECs.

Overall, as κ-CA fibers exhibit high swelling ratios, the weakening of the network occurred and, consequently, cells were able to escape from the fibers. CHT coating maintained the fiber diameter, delaying their disintegration and the consequent release of cells into the surrounding environment. Nonetheless,

dx.doi.org/10.1021/bm500036a | Biomacromolecules XXXX, XXX, XXX−XXX

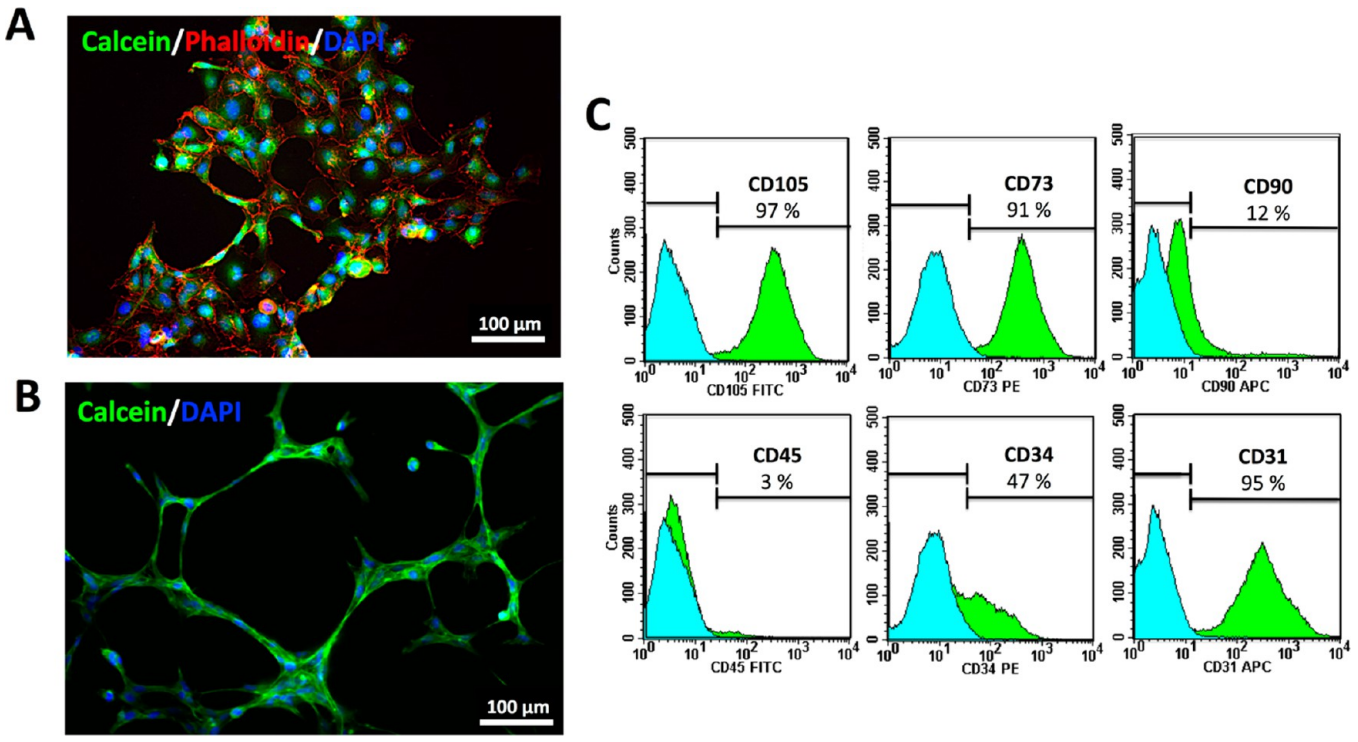

Figure 7. Endothelial phenotype of cells retrieved from the fibers after 21 days of culture. (A) After retrieval of cells through degradation of the fibers, and their subsequent seeding, cells adhered and formed small colonies, characterized by close contact between cells (live/cytoskeleton/nuclei). (B) Cells maintained their ability to form tubular-like structures (green) when seeded on Matrigel (C) and the expression of the initial endothelial phenotype-associated panel of markers. Cell nuclei were counterstained with DAPI (blue).

the CHT layer was still permissive to culture medium, allowing the diffusion of its components, as suggested by the subsequent remarkable results concerning the viability and phenotype of encapsulated cells. These findings further demonstrate the potential of using these fibers as EC carriers within different TE constructs.

3.5. Cell-Loaded κ-CA-Based Fibers Can Act as Building Blocks within 3D Hydrogel Constructs. In vitro 3D co-culture platforms provide a scalable and flexible approach to evaluate the indirect interactions between multiple-cell types in highly defined settings, enabling us to address specific cellular behaviors and the formation of complex tissue-like analogs. Simultaneously, the integration and assembly of cell-laden templates as building blocks within 3D constructs may allow the development of replicas of complex tissues to use in TE approaches. Herein, we proposed a straightforward method to integrate the κ-CA-based fibers enclosing SSEA-4$^+$hASCs-derived ECs, within a 3D hydrogel containing SSEA-4$^+$hASCs-derived osteoblast-like cells, as heterotypic constructs of interest for bone TE. Within this approach, we took advantage of the ease preparation of cell-loaded κ-CA fibers, to recreate the cellular indirect communication at a 3D scale. Thus, cell-loaded fibers, used as building blocks, were assembled within a κ-CA hydrogel disc by simply laying them in a Petri dish (Figure 8). They could be singled out or stacked in a random or organized manner (Figure 8A). When the cell-laden fibers were integrated in a hydrogel disc containing osteoblast-like cells, the formation of a 3D heterotypic platform with a defined cellular topography suitable for bone-vascularization strategies was achieved (Figure 8B–C). The proposed system was entirely formed by a κ-CA matrix, with a controlled spatial distribution of the two cell types derived from the same source. The fibers are expected to act both as cell-reservoirs and structurally defined arrangements in the surrounding matrix. Within the context of bone TE, further experiments aim to deeply assess the cellular interactions within the 3D structure and the consequent outcome, both concerning the outflow of ECs triggered by the crosstalk with osteoblast cells,[60,61] as well as osteogenic matrix deposition and mineralization. This could eventually lead to the organization of ECs within the osteoblast-containing matrix, leading to an improvement in the osteogenic outcome.

For the immediate integration of fibers in a secondary matrix, the CHT coating does not provide additional advantages, as the secondary matrix will already hold the fibers in place. Nevertheless, the CHT coating proves to be crucial for prolonged culture periods that are relevant when using this approach to study indirect interactions between multiple-cell types and/or for those 3D systems in which the accuracy of the initial parameters (shape, size, swelling, mechanical stability) is crucial. For instance, it could be possible to create a 3D co-culture system based on coated cell-laden κ-CA fibers by seeding another cell type on top of the fibers.

4. CONCLUSIONS

The development of chitosan (CHT) reinforced κ-carrageenan (κ-CA) fibers using a two-step procedure, under cell-friendly experimental settings, aiming at homogeneous immobilization of cells is herein reported. The diameter of the fibers could be easily tuned by selecting the appropriate needle gauge during processing. The presence of the CHT coating enhanced the stability of the fibers and their diameter was maintained constant by restraining their swelling. Moreover, these fibers support the viability and functionality of encapsulated cells during long-term culturing, enabling their use as cell-delivery systems within 3D

dx.doi.org/10.1021/bm500036a | Biomacromolecules XXXX, XXX, XXX−XXX

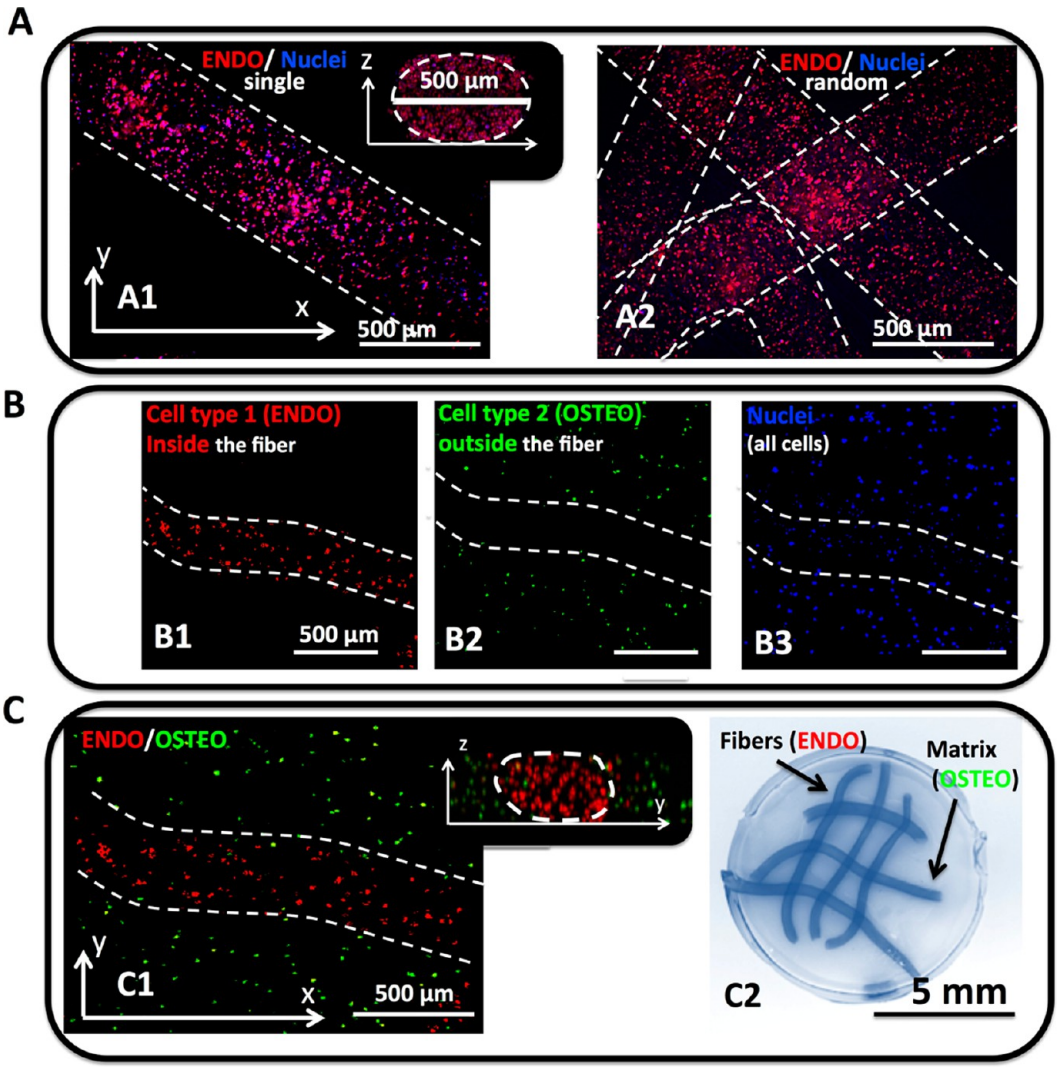

Figure 8. Proof of concept of the use of cell-loaded κ-CA-based fibers as building blocks within 3D κ-CA hydrogel constructs. Confocal laser scanning micrographs of (A1−2) encapsulated SSEA-4+hASCs-derived ECs (ENDO) within κ-CA fibers. Fibers can be (A1) singled out or (A2) randomly stacked. (B,C) Heterotypic 3D κ-CA-based structure. (B) The encapsulation of ENDO preceded the integration of the fibers within the κ-CA containing the SSEA-4+hASCs-derived osteoblast-like cells (OSTEO) localized outside the fiber. All cells (blue) were evenly distributed within the hydrogel. (C) 3D buildup of fiber stacks within a hydrogel disc consisted of a controlled spatial localization of two cell types within a single hydrogel matrix. (C1) The colocalization of ENDO and OSTEO is relevant for developing spatial controlled heterotypic systems aimed at vascularized bone TE approaches. Cell nuclei were counterstained with DAPI (blue). (C2) A macroscopic view of the 3D construct. The discs were manually manipulated without damage. κ-CA fibers were stained with methylene blue (dark blue).

tissue engineering constructs. Furthermore, using a bottom-up approach, these fibers can be used as building blocks for the development of suitable 3D platforms of independently organized heterotypic cell-containing hydrogels, relevant for TE approaches.

■ ASSOCIATED CONTENT

Supporting Information

Supplemental figures depict the endothelial phenotype of SSEA-4^{+}hASCs-derived ECs phenotype prior encapsulation and the propidium iodide/DAPI images of fibers along time as well as the quantification of the cellular viability. This material is available free of charge via the Internet at http://pubs.acs.org.

■ AUTHOR INFORMATION

Corresponding Author

*E-mail: megomes@dep.uminho.pt.

Notes

The authors declare no competing financial interest.

■ ACKNOWLEDGMENTS

Authors thank the Portuguese Foundation for Science and Technology (FCT) for the personal grants SFRH/BD/42968/2008 through the MIT-Portugal Program (SMM) and SFRH/BD/64070/2009 (EGP). The research leading to these results has received funding from the European Union's Seventh Framework Programme (FP7/2007-2013) under grant agreement no REGPOT-CT2012-316331-POLARIS and MIT/ECE/0047/2009 project.

■ REFERENCES

(1) Berthiaume, F.; Maguire, T. J.; Yarmush, M. L. Tissue engineering and regenerative medicine: history, progress, and challenges. *Annu. Rev. Chem. Biomol. Eng.* **2011**, *2*, 403−30.

(2) Kannan, R. Y.; Salacinski, H. J.; Sales, K.; Butler, P.; Seifalian, A. M. The roles of tissue engineering and vascularisation in the development of micro-vascular networks: a review. *Biomaterials* **2005**, *26* (14), 1857–75.
(3) Bae, H.; Puranik, A. S.; Gauvin, R.; Edalat, F.; Carrillo-Conde, B.; Peppas, N. A.; Khademhosseini, A. Building vascular networks. *Sci. Transl. Med.* **2012**, *4* (160), 160ps23.
(4) Lovett, M.; Lee, K.; Edwards, A.; Kaplan, D. L. Vascularization strategies for tissue engineering. *Tissue Eng., Part B* **2009**, *15* (3), 353–70.
(5) Phelps, E. A.; Garcia, A. J. Engineering more than a cell: vascularization strategies in tissue engineering. *Curr. Opin. Biotechnol.* **2010**, *21* (5), 704–9.
(6) Geckil, H.; Xu, F.; Zhang, X.; Moon, S.; Demirci, U. Engineering hydrogels as extracellular matrix mimics. *Nanomedicine* **2010**, *5* (3), 469–84.
(7) Drury, J. L.; Mooney, D. J. Hydrogels for tissue engineering: scaffold design variables and applications. *Biomaterials* **2003**, *24* (24), 4337–51.
(8) Malafaya, P. B.; Silva, G. A.; Reis, R. L. Natural-origin polymers as carriers and scaffolds for biomolecules and cell delivery in tissue engineering applications. *Adv. Drug Delivery Rev.* **2007**, *59* (4–5), 207–33.
(9) Fedorovich, N. E.; Wijnberg, H. M.; Dhert, W. J.; Alblas, J. Distinct tissue formation by heterogeneous printing of osteo- and endothelial progenitor cells. *Tissue Eng., Part A* **2011**, *17* (15–16), 2113–21.
(10) Kang, E.; Jeong, G. S.; Choi, Y. Y.; Lee, K. H.; Khademhosseini, A.; Lee, S. H. Digitally tunable physicochemical coding of material composition and topography in continuous microfibres. *Nat. Mater.* **2011**, *10* (11), 877–83.
(11) Aubin, H.; Nichol, J. W.; Hutson, C. B.; Bae, H.; Sieminski, A. L.; Cropek, D. M.; Akhyari, P.; Khademhosseini, A. Directed 3D cell alignment and elongation in microengineered hydrogels. *Biomaterials* **2010**, *31* (27), 6941–6951.
(12) Liu, Y.; Sakai, S.; Taya, M. Production of endothelial cell-enclosing alginate-based hydrogel fibers with a cell adhesive surface through simultaneous cross-linking by horseradish peroxidase-catalyzed reaction in a hydrodynamic spinning process. *J. Biosci. Bioeng.* **2012**, *114* (3), 353–9.
(13) Takei, T.; Sakai, S.; Ijima, H.; Kawakami, K. Development of mammalian cell-enclosing calcium-alginate hydrogel fibers in a co-flowing stream. *Biotechnol. J.* **2006**, *1* (9), 1014–7.
(14) Sakai, S.; Yamaguchi, S.; Takei, T.; Kawakami, K. Oxidized alginate-cross-linked alginate/gelatin hydrogel fibers for fabricating tubular constructs with layered smooth muscle cells and endothelial cells in collagen gels. *Biomacromolecules* **2008**, *9* (7), 2036–41.
(15) Enea, D.; Henson, F.; Kew, S.; Wardale, J.; Getgood, A.; Brooks, R.; Rushton, N. Extruded collagen fibres for tissue engineering applications: effect of crosslinking method on mechanical and biological properties. *J. Mater. Sci. Mater. Med.* **2011**, *22* (6), 1569–78.
(16) Oliveira, J. T.; Martins, L.; Picciochi, R.; Malafaya, P. B.; Sousa, R. A.; Neves, N. M.; Mano, J. F.; Reis, R. L. Gellan gum: a new biomaterial for cartilage tissue engineering applications. *J. Biomed. Mater. Res., Part A* **2010**, *93* (3), 852–63.
(17) Berger, J.; Reist, M.; Mayer, J. M.; Felt, O.; Peppas, N. A.; Gurny, R. Structure and interactions in covalently and ionically crosslinked chitosan hydrogels for biomedical applications. *Eur. J. Pharm. Biopharm.* **2004**, *57* (1), 19–34.
(18) Popa, E. G.; Gomes, M. E.; Reis, R. L. Cell delivery systems using alginate–carrageenan hydrogel beads and fibers for regenerative medicine applications. *Biomacromolecules* **2011**, *12* (11), 3952–61.
(19) Kirsch, P. P. Carrageenan: a safe additive. *Environ. Health Perspect.* **2002**, *110* (6), A288 author reply A288..
(20) Popa, E. G.; Reis, R. L.; Gomes, M. E. Chondrogenic phenotype of different cells encapsulated in kappa-carrageenan hydrogels for cartilage regeneration strategies. *Biotechnol. Appl. Biochem.* **2012**, *59* (2), 132–41.
(21) Popa, E. G.; Rodrigues, M. T.; Coutinho, D. F.; Oliveira, M. B.; Mano, J. F.; Reis, R. L.; Gomes, M. E. Cryopreservation of cell laden natural origin hydrogels for cartilage regeneration strategies. *Soft Matter* **2013**, *9* (3), 875–885.
(22) Santo, V. E.; Frias, A. M.; Carida, M.; Cancedda, R.; Gomes, M. E.; Mano, J. F.; Reis, R. L. Carrageenan-based hydrogels for the controlled delivery of PDGF-BB in bone tissue engineering applications. *Biomacromolecules* **2009**, *10* (6), 1392–401.
(23) Salgueiro, A. M.; Daniel-da-Silva, A. L.; Fateixa, S.; Trindade, T. kappa-Carrageenan hydrogel nanocomposites with release behavior mediated by morphological distinct Au nanofillers. *Carbohydr. Polym.* **2013**, *91* (1), 100–9.
(24) Kuo, C. K.; Ma, P. X. Maintaining dimensions and mechanical properties of ionically crosslinked alginate hydrogel scaffolds in vitro. *J. Biomed. Mater. Res., Part A* **2008**, *84* (4), 899–907.
(25) Mihaila, S. M.; Gaharwar, A. K.; Reis, R. L.; Marques, A. P.; Gomes, M. E.; Khademhosseini, A. Photocrosslinkable kappa-carrageenan hydrogels for tissue engineering applications. *Adv. Healthcare Mater.* **2013**, *2* (6), 895–907.
(26) Hezaveh, H.; Muhamad, I. I.; Noshadi, I.; Shu Fen, L.; Ngadi, N. Swelling behaviour and controlled drug release from cross-linked kappa-carrageenan/NaCMC hydrogel by diffusion mechanism. *J. Micro-encapsulation* **2012**, *29* (4), 368–79.
(27) Amici, E.; Clark, A. H.; Normand, V.; Johnson, N. B. Interpenetrating network formation in agarose–kappa-carrageenan gel composites. *Biomacromolecules* **2002**, *3* (3), 466–74.
(28) Granero, A. J.; Razal, J. M.; Wallace, G. G.; Panhuis, M. i. h. Conducting gel-fibres based on carrageenan, chitosan and carbon nanotubes. *J. Mater. Chem.* **2010**, *20*, 7953–7956.
(29) Colinet, I.; Dulong, V.; Mocanu, G.; Picton, L.; Le Cerf, D. Effect of chitosan coating on the swelling and controlled release of a poorly water-soluble drug from an amphiphilic and pH-sensitive hydrogel. *Int. J. Biol. Macromol.* **2010**, *47* (2), 120–5.
(30) Chang, H. H.; Wang, Y. L.; Chiang, Y. C.; Chen, Y. L.; Chuang, Y. H.; Tsai, S. J.; Heish, K. H.; Lin, F. H.; Lin, C. P. A novel chitosan-gammaPGA polyelectrolyte complex hydrogel promotes early new bone formation in the alveolar socket following tooth extraction. *PLoS One* **2014**, *9* (3), e92362.
(31) Grenha, A.; Gomes, M. E.; Rodrigues, M.; Santo, V. E.; Mano, J. F.; Neves, N. M.; Reis, R. L. Development of new chitosan/carrageenan nanoparticles for drug delivery applications. *J. Biomed. Mater. Res., Part A* **2010**, *92* (4), 1265–72.
(32) Piyakulawat, P.; Praphairaksit, N.; Chantarasiri, N.; Muangsin, N. Preparation and evaluation of chitosan/carrageenan beads for controlled release of sodium diclofenac. *AAPS PharmSciTech* **2007**, *8* (4), E97.
(33) Pinheiro, A. C.; Bourbon, A. I.; Medeiros, B. G. d. S.; Silva, L. s. H. M. d.; Silva, M. C. H. d.; Carneiro-da-Cunha, M. G.; Coimbra, M. A.; Vicente, A. n. A. Interactions between k-carrageenan and chitosan in nanolayered coatings—Structural and transport properties. *Carbohydr. Polym.* **2012**, *87*, 1081–1090.
(34) Mihaila, S. M.; Frias, A. M.; Pirraco, R. P.; Rada, T.; Reis, R. L.; Gomes, M. E.; Marques, A. P. Human adipose tissue-derived SSEA-4 subpopulation multi-differentiation potential towards the endothelial and osteogenic lineages. *Tissue Eng., Part A* **2013**, *19* (1–2), 235–46.
(35) Signini, R.; Filho, S. P. C. Characteristics and properties of purified chitosan in the neutral, acetate and hydrochloride forms. *Polím. Ciênc. Tecnol.* **2001**, *11*, 58–64.
(36) Cho, J.; Heuzey, M. C.; Begin, A.; Carreau, P. J. Physical gelation of chitosan in the presence of beta-glycerophosphate: the effect of temperature. *Biomacromolecules* **2005**, *6* (6), 3267–75.
(37) Huh, D.; Hamilton, G. A.; Ingber, D. E. From 3D cell culture to organs-on-chips. *Trends Cell Biol.* **2011**, *21* (12), 745–54.
(38) Hahn, M. S.; Miller, J. S.; West, J. L. Three-dimensional biochemical and biomechanical patterning of hydrogels for guiding cell behavior. *Adv. Mater.* **2006**, *18* (20), 2679–2684.
(39) Oliveira, J. T.; Gardel, L. S.; Rada, T.; Martins, L.; Gomes, M. E.; Reis, R. L. Injectable gellan gum hydrogels with autologous cells for the treatment of rabbit articular cartilage defects. *J. Orthop. Res.* **2010**, *28* (9), 1193–9.

(40) Kim, I. L.; Khetan, S.; Baker, B. M.; Chen, C. S.; Burdick, J. A. Fibrous hyaluronic acid hydrogels that direct MSC chondrogenesis through mechanical and adhesive cue. *Biomaterials* **2013**, *34* (22), 5571−80.
(41) Popa, E. G.; Caridade, S. G.; Mano, J. F.; Reis, R. L.; Gomes, M. E. Chondrogenic potential of injectable kappa-carrageenan hydrogel with encapsulated adipose stem cells for cartilage tissue-engineering applications. *J. Tissue Eng. Regen. Med.* **2013**, DOI: 10.1002/term.1683.
(42) Pereira, R. C.; Scaranari, M.; Castagnola, P.; Grandizio, M.; Azevedo, H. S.; Reis, R. L.; Cancedda, R.; Gentili, C. Novel injectable gel (system) as a vehicle for human articular chondrocytes in cartilage tissue regeneration. *J. Tissue Eng. Regen. Med.* **2009**, *3* (2), 97−106.
(43) Fedorovich, N. E.; De Wijn, J. R.; Verbout, A. J.; Alblas, J.; Dhert, W. J. Three-dimensional fiber deposition of cell-laden, viable, patterned constructs for bone tissue printing. *Tissue Eng., Part A* **2008**, *14* (1), 127−33.
(44) Coutinho, D. F.; Sant, S. V.; Shin, H.; Oliveira, J. T.; Gomes, M. E.; Neves, N. M.; Khademhosseini, A.; Reis, R. L. Modified Gellan Gum hydrogels with tunable physical and mechanical properties. *Biomaterials* **2010**, *31* (29), 7494−502.
(45) Stephen, A. M.; Phillips, G. O.; Williams, P. A. *Food Polysaccharides and their Applications*, 2nd ed.; Press, C., Ed.; Taylor & Francis Group: New York, 2006.
(46) Polk, A.; Amsden, B.; De Yao, K.; Peng, T.; Goosen, M. F. Controlled release of albumin from chitosan-alginate microcapsules. *J. Pharm. Sci.* **1994**, *83* (2), 178−85.
(47) Naciri, M.; Kuystermans, D.; Al-Rubeai, M. Monitoring pH and dissolved oxygen in mammalian cell culture using optical sensors. *Cytotechnology* **2008**, *57* (3), 245−50.
(48) Baker, L. G.; Specht, C. A.; Donlin, M. J.; Lodge, J. K. Chitosan, the deacetylated form of chitin, is necessary for cell wall integrity in Cryptococcus neoformans. *Eukaryotic Cell* **2007**, *6* (5), 855−67.
(49) Popa, E. G.; Carvalho, P. P.; Dias, A. F.; Santos, T. C.; Santo, V. E.; Marques, A. P.; Viegas, C. A.; Dias, I. R.; Gomes, M. E.; Reis, R. L. Evaluation of the in vitro and in vivo biocompatibility of carrageenan-based hydrogels. *J. Biomed. Mater. Res., Part A* **2014**, DOI: 10.1002/jbm.a.35081.
(50) Popa, E.; Reis, R.; Gomes, M. Chondrogenic phenotype of different cells encapsulated in kappa-carrageenan hydrogels for cartilage regeneration strategies. *Biotechnol. Appl. Biochem.* **2012**, *59* (2), 132−41.
(51) Fedorovich, N. E.; Haverslag, R. T.; Dhert, W. J.; Alblas, J. The role of endothelial progenitor cells in prevascularized bone tissue engineering: development of heterogeneous constructs. *Tissue Eng., Part A* **2010**, *16* (7), 2355−67.
(52) Urbich, C.; Dimmeler, S. Endothelial progenitor cells: characterization and role in vascular biology. *Circulation Res.* **2004**, *95* (4), 343−53.
(53) Kong, H. J.; Smith, M. K.; Mooney, D. J. Designing alginate hydrogels to maintain viability of immobilized cells. *Biomaterials* **2003**, *24* (22), 4023−9.
(54) Lutolf, M. P.; Gilbert, P. M.; Blau, H. M. Designing materials to direct stem-cell fate. *Nature* **2009**, *462* (7272), 433−41.
(55) Bryant, S. J.; Anseth, K. S. The effects of scaffold thickness on tissue engineered cartilage in photocrosslinked poly(ethylene oxide) hydrogels. *Biomaterials* **2001**, *22* (6), 619−26.
(56) Park, J. H.; Chung, B. G.; Lee, W. G.; Kim, J.; Brigham, M. D.; Shim, J.; Lee, S.; Hwang, C. M.; Durmus, N. G.; Demirci, U.; Khademhosseini, A. Microporous cell-laden hydrogels for engineered tissue constructs. *Biotechnol. Bioeng.* **2010**, *106* (1), 138−48.
(57) Bai, Z.; Mendoza Reyes, J. M.; Montazami, R.; Hashemi, N. On-chip development of hydrogel microfibers from round to square/ribbon shape. *J. Mater. Chem. A* **2014**, *2*, 4878−4884.
(58) Adams, C. S.; Mansfield, K.; Perlot, R. L.; Shapiro, I. M. Matrix regulation of skeletal cell apoptosis. Role of calcium and phosphate ions. *J. Biol. Chem.* **2001**, *276* (23), 20316−22.
(59) Murphy, C. L.; Sambanis, A. Effect of oxygen tension and alginate encapsulation on restoration of the differentiated phenotype of passaged chondrocytes. *Tissue Eng.* **2001**, *7* (6), 791−803.
(60) Pirraco, R. P.; Melo-Ferreira, B.; Santos, T. C.; Frias, A. M.; Marques, A. P.; Reis, R. L. Adipose stem cell-derived osteoblasts sustain the functionality of endothelial progenitors from the mononuclear fraction of umbilical cord blood. *Acta Biomater.* **2013**, *9* (2), 5234−42.
(61) Pirraco, R. P.; Marques, A. P.; Reis, R. L. Cell interactions in bone tissue engineering. *J. Cell. Mol. Med.* **2010**, *14* (1−2), 93−102.